Dynamics of Anthracene Excimer Formation within a Water-soluble Nanocavity at Room Temperature

Journal:	*Journal of the American Chemical Society*
Manuscript ID	ja-2020-10093w
Manuscript Type:	Article
Date Submitted by the Author:	21-Sep-2020
Complete List of Authors:	Das, Aritra; Indian Institute of Technology Kanpur, Department of Chemistry Danao, Ashwini; University of Miami, Chemistry Mohan Raj, Anthony Raj; Univeristy of Miami, Chemistry Sharma, Gaurav; University of Miami, Department of Chemistry Banerjee, Shubhojit ; IISER, Chemistry Prabhakar, Rajeev; University of Miami, Chemistry Srinivasan, Varadharajan; Indian Institute of Science Education and Research Bhopal, Chemistry Ramamurthy, Vaidhyanathan; University of Miami, Chemistry; Sen, Pratik; Indian Institute of Technology Kanpur, Department of Chemistry

Dynamics of Anthracene Excimer Formation within a Water-soluble Nanocavity at Room Temperature

Aritra Das, Ashwini Danao, A. Mohan Raj, Gaurav Sharma, Shubhojit Banerjee, Rajeev Prabhakar, Varadharajan Srinivasan,* V. Ramamurthy* and Pratik Sen*

Department of Chemistry, Indian Institute of Technology Kanpur, Kanpur – 208 016, UP, India
Department of Chemistry, University of Miami, Coral Gables, Florida 33146, United States
Department of Chemistry, Indian Institute of Science Education and Research Bhopal, Bhopal 462 066, India

Abstract

Excited anthracene is well-known to photodimerize in solution and not to exhibit excimer emission. In this report we outline a strategy by which the excited state behavior of this exemplar molecule can be reversed in aqueous solution at room temperature. Anthracene forms two types of supramolecular hots-guest complexes (1:2 and 2:2, G:H) with the synthetic host octa acid in an aqueous medium. Excitation of the 2:2 complex results in intense excimer emission, a phenomenon thus far unknown. Furthermore, time resolved emission experiments revealed the excimer emission maximum to be time dependent. This observation is unique and not in line with the textbook examples of monomer-excimer emissions of aromatics in solution. Presence of at least one intermediate between the monomer and the excimer is inferred from time-resolved area normalized emission spectra. Potential energy curves calculated for ground and excited states of anthracene via QM/MM-TDDFT method supports the model proposed based on experimental observations. Results presented here on the excited state behavior of a well investigated aromatic molecule anthracene establish that the behavior of a molecule is likely to drastically change under confinement. Analogy with biological systems is obvious.

Introduction

Anthracene (AN) and pyrene (PY) occupy a special place in the history of the photochemistry[1-2] and photophysics[3-4] of aromatic molecules. The concepts that currently prevail concerning the excited state chemistry of aromatic molecules could be traced back to these two molecules serving as exemplars in the development of concepts related to excimers and photodimerizations.[1-2, 5-7] AN is well-known, even a century ago, to photodimerize with a limiting quantum yield of one in solution at room temperature.[1-2] On the other hand, PY does not dimerize under any conditions. However, it shows an emission in addition to fluorescence and phosphorescence in solution at room temperature even at 10^{-4} M.[3] The intense concentration and temperature dependent emission of PY with a lifetime of 90 ns[8] initially recorded by Forster and Kasper is currently known to originate from excimer (excited state dimer). In contrast, AN that photodimerizes from excited singlet state mainly fluoresce and phosphoresce in solution.[3] Recognizing the anomaly between AN and PY, Chandross devised an ingenious method by which excimer emission from anthracene could be recorded at 77 °K in an organic glass.[9-11] He generated sandwich dimers (two AN molecules placed side by side with long and short axis parallel to each other) via photolytic decomposition of dianthracene (dimer of AN; Scheme 1), which upon excitation gave intense broad emission red shifted with respect to fluorescence. This was attributed to excimer and found to have a long lifetime (~ 185–225 ns).[12-15] Following this, Ferguson showed that excimer emission could be recorded in crystalline state as well as in KBr matrix by following the above procedure.[16-19] As expected, the excitation spectrum corresponded to the absorption spectrum of AN monomer. While the sandwich dimer showed intense excimer emission at 77 K, upon warming the matrix the excimer emission disappeared and the dimer dianthracene was formed with near unit quantum yield at room temperature.[20] The above observations made it clear that excimer is an intermediate en-route to photodimer. It is clear that to record excimer emission from AN two criteria need to be fulfilled: (a) two molecules of anthracene should be brought closer with some free space around them so that they could explore various orientations,[21] (b) the barrier for dimerization should be increased by the surroundings and (c) temperature of irradiation should be controlled so that the required energy is not available to overcome the barrier by the excimer to proceed to dimer. In this context supramolecular encapsulation can be as effective as low temperature and hard matrix.[5, 22] Supramolecular hosts such as micelles and cavitands can increase the local concentration as well as offer barriers for

molecular transformations. Following the initial report of Forster and Selinger on 2-methyl naphthalene and PY in micelles,[23] the literature is replete with examples where excimer emission is reported at low concentrations in micelles and cyclodextrins.[24-31] However, as far we are aware, excimer emission from AN has not been achieved within supramolecular assemblies in solution at any temperatures.

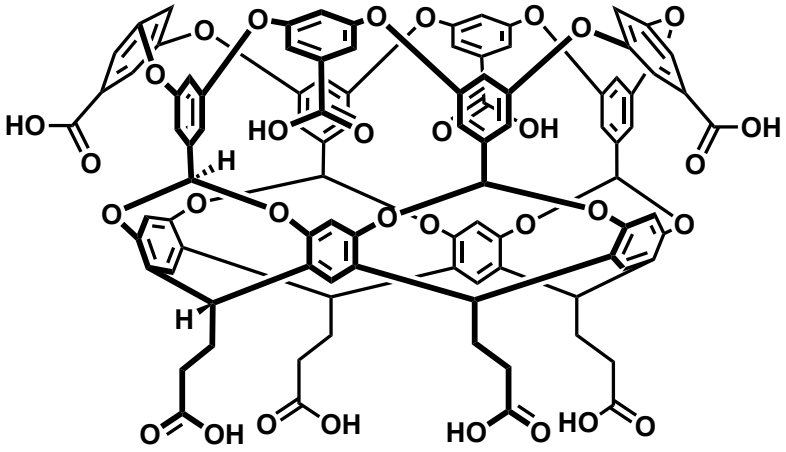

Octa acid (OA)

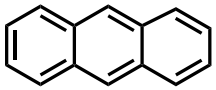

Anthracene (AN)

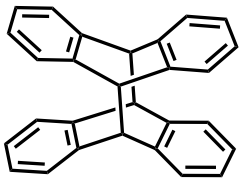

Dianthracene

Scheme 1. Structures of host OA, guest anthracene and the dianthracene from which anthracene sandwich dimer is generated.

Having recorded excimer emission from PY in solution at room temperature and knowing the location and shape of the excimer emission spectrum of AN from the work of Chandross and Ferguson, several workers searched for AN excimer emission in solution at room temperature.[32-35] Results have been mixed. An early report suggested the formation of AN excimer (λ_{max}: 520 nm) in glycerol solution at room temperature during triplet-triplet annihilation.[32] Next two studies were unable to detect emission but suggested the presence of excimer in solution through its transient absorption in the IR region (half-life of 3 ns) and singlet-singlet quenching by rhodamine B (lifetime: 1.5 ns).[33-34] In a later study a full spectrum recorded at 0.2 M AN in

chloroform at 305 K showed both structured (350-470 nm) and broad emissions (480-600 nm).[35] The latter with a lifetime of 1.45±0.22 ns was attributed to excimer. A different group by measuring the rise time of the broad emission (710 ± 30 ps) supported the claim that the weak broad emission is indeed due to excimer.[36] Finally, liquid AN, formed by melting crystalline AN, was found to show excimer emission with a lifetime of 0.2 ns and rise time of 100 ps.[37] Based on above studies one can conclude that AN excimer emission in solution is very weak (if at all), has a short lifetime (< 2 ns, compare with lifetime at 77 K > 200 ns) and recording it is not trivial. This is quite different from what happens at low temperature when the pre-prepared sandwich dimer of AN is excited. The contrast suggested to us that if we could confine two molecules of anthracene in a small space and close the pathway to dimerization by supramolecular steric features of the host, we should be able to record the excimer emission at room temperature in solution.

In this report, we present our results on excimer emission from AN in aqueous solution at room temperature with the help of octa acid cavitand (OA, Scheme 1) that encapsulates two molecules of AN by forming a capsular assembly (2:2 host-guest complex).[38-39] The capsule not only enhances the local concentration but also increases the barrier for dimer formation. The comprehensive undertaking includes host-guest complexation studies by NMR, molecular dynamics simulation of the host-guest structure, ultrafast time resolved experiments to follow the dynamics in the excited state and quantum chemical calculations that map the excited state surface from monomer to excimer. Given the history of attempts to record anthracene excimer emission in solution, our ability to routinely record excimer emission at 10^{-5} M of AN in water is remarkable and display the future potential of this method in recording emission from non-emissive excimers in solution.[40] Results discussed below make a valuable addition to our fundamental understanding of the excited state dynamics of an exemplar molecule AN in a confined space.

Experimental

Materials: The host octa acid was synthesized following the published procedure.[38] Anthracene (Sigma-Aldrich) was recrystallized from ethanol before use. Deuterated anthracene

from MSD Isotopes was used as received. Deuterated water from Sigma-Aldrich was used as received. Sodium borate buffer from Sigma was used as received. Spectroscopic grade solvents were used for absorption and emission studies. Double distilled water was used throughout the study.

NMR studies: A D_2O solution (600 μL) of host OA (1 mM OA in 10 mM $Na_2B_4O_7$) was taken in a NMR tube and was added 0.1 equivalent increment of AN (1.0 μL of a 60 mM solution in DMSO-d_6). The ^{1}H NMR experiments were carried out after sonicating the NMR tube for 15 min after each addition. Titration experiment was repeated with per deuterated AN in order to identify the guest resonances. ^{1}H NMR spectra were recorded using Bruker 500 MHz NMR spectrometer at 25 ^{0}C in deuterated water under aerated conditions.

Steady-state and time-resolved emission studies: UV−visible absorption spectra were recorded in UV-2450, Shimadzu, Japan and all the fluorescence spectra were recorded in Fluoromax-4, Jobin-Yvon, USA. AN stock solution (1 mM) was prepared in spectrophotometric grade methanol. Appropriate amount of AN stock was added to sodium borate buffer solution so that the concentration of anthracene become 5 μM. To this solution, 0.2 equivalent increments of OA (2 μL of 1 mM OA in 10 mM sodium borate buffer) was added until 2.0 equivalent to observe $AN_2@OA_2$ excimer formation. To this solution, further addition of OA continued until 10.0 equivalent to observe $AN@OA_2$ monomer formation. The emission spectra were recorded by exciting at 350 nm. Time-resolved fluorescence were collected using a commercial time correlated single photon counting setup (Life Spec II, Edinburgh Instruments, UK) under magic angle condition. All samples were excited at 375 nm pulsed diode laser source, and the full width at the half-maxima of the instrument response function (IRF) is 120 ps. The fluorescence transients were analyzed by deconvoluting with the IRF and fitted with a sum of two exponentials for the present study.

Femtosecond transient absorption study: The time resolved data were acquired on a commercial femtosecond transient absorption spectroscopy setup (FemtoFrame-II, IB Photonics, Bulgaria). The details of the setup are described earlier[41] and only a brief overview is presented here. The fundamental 800 nm light was obtained from a Ti-Sapphire regenerative amplifier (Spitfire Pro XP, Spectra-Physics, USA) pumped by a 20-W Q-switched Nd:YLF laser (Empower, Spectra-Physics, USA) and seeded with a Ti-Sapphire femtosecond oscillator

(MaiTai SP, Spectra-Physics, USA). The fundamental light thus obtained was divided into two parts. One part was passed through a β-barium borate (BBO) crystal to generate the 400 nm light, which was used as pump pulse. The other part of the beam was passed through a delay stage, having a maximum delay time of 2 ns, and focused on a sapphire crystal to generate the white light continuum, which was used as the probe light. After passing through the sample the probe light was dispersed in polychromator and detected using a CCD. For all experiments the power of the pump light was kept ~10 μW. The pulse width of the fundamental light was 80 fs and the instrument response function was measured to be 150 fs. The kinetics at a particular wavelength was fitted with sum of two exponential functions after deconvoluting the Gaussian shaped instrument response function with 150 fs FWHM.

Computational Details: Molecular dynamics (MD) simulations were performed using the following multi-step strategy. In the first step, a three-dimensional structure of OA was taken from our previous work[42] and optimized using the Gaussian 09 program.[43] The initial structure of anthracene was built using the Gaussview program and optimized without any geometrical constraints at the B3LYP[44]/6-31g(d)[45] level utilizing the Gaussian 09 program. Antechamber, an inbuilt tool in Amber, was used to calculate RESP charges and for making topology files of all molecules.[46] Autodock Vina 1.5.6 software was used to perform molecular docking that provided initial binding poses of anthracene on OA.[47] In this procedure, the grid size was chosen to cover the entire OA and spacing was kept to 1.00 Å, which is a standard value for Autodock Vina. The all-atom MD simulations of the OA-anthracene complexes were performed using the GROMACS[48] program utilizing the AMBER03[49] force field. The starting structures were placed in a cubic box of dimensions (60 × 60 × 60 Å^3) filled with TIP3P water molecules.[50] Some of the water molecules were replaced with the Na^+ ions to neutralize the system. Energy minimizations of the OA-anthracene complexes were performed for 3000 steps by the steepest descent method that resulted in the formation of the starting structures for the subsequent 100 ns all-atom MD simulations in an aqueous solution. The simulations were carried out with a constant number of particles (N), pressure (P), and temperature (T) i.e. NPT ensemble. The bond lengths and angles of the water molecules were constrained by the SETTLE[51] algorithm and the LINCS[52] algorithm was used to constrain the bond lengths of the OA. Particle-Mesh Ewald (PME) method was used to calculate the long-range electrostatic interactions. A MD trajectory was computed for each model with a time step of 2 fs. Cluster analysis was performed to derive the most representative

structure of a particular trajectory. Yasara[53] and Chimera[54] programs were used for visualization and the preparation of the structural diagrams presented in this study.

Considering the large size of the system (432 atoms for the $AN_2@OA_2$ complex), we employed a mixed QM/MM [Warshel *et al.* 1976] approach to explore the mechanism of excimer formation. The quantum mechanical (QM) calculations used density-functional theory (DFT) for ground and time-dependent DFT (TDDFT) for excited states as implemented in the NWChem code.[55] The Anthracene molecules were modeled in the QM region using the CAM-B3LYP functional[56] along with the BJ-damped[57] Grimme's D3 dispersion[58] and a 6-31G(d,p) basis set. The OA cage was treated with Molecular Mechanics using the AMBER03[48] force field. For the purposes of the electronic structure calculations, a charge neutral version of the OA was used by saturating all the carboxylate ends with H atoms and relaxing H atom positions keeping the rest of the molecule fixed in the MD averaged geometry.

The total QM/MM energy of the system was calculated as $E_{QM/MM} = E_{QM} + E_{MM} + E_{QM\text{-}MM}$, where E_{QM} is the Quantum mechanical energy of the QM part, E_{MM} is the energy for the MM region at the force field level, $E_{QM\text{-}MM}$ is the interaction energy between the QM and MM part. QM/MM TD-DFT was performed to calculate the excitation energies at various points. We carried out QM/MM optimization of the complex by constraining the geometry of the MM part to an average structure obtained from the MD simulations and only allowing the QM part to move. Potential energy curves (PEC) were calculated by rigidly displacing the confined AN molecules in opposite directions along the perpendicular to their planes (*a*), short-axis (*b*) and long-axis (*c*), respectively, starting from their optimized positions. Binding energies for the anthracene dimer for different displacements in the OA cage were computed as

$$E_{\text{binding}} = E_{\text{complex}}(\text{QM/MM}) - E_{\text{OA}}(\text{MM}) - 2\,E_{\text{AN}}(\text{QM})$$

where $E_{complex}$ (QM/MM) is defined above**,** $E_{\mathbf{OA}}$(MM) is the classical energy of the OA cage and E_{AN}(QM) is the DFT energy of the gas-phase optimized AN molecule. The PEC plots discussed below use the binding energy of the optimized complex as a reference.

Results and Discussion

The current study focused on establishing the feasibility of recording excimer emission from anthracene at room temperature includes monitoring host-guest complexation by NMR spectroscopy, time resolved experiments to observe the dynamics of excimer formation, quantum chemical calculations to map out the excited state potential energy surface between monomer and excimer and molecular dynamics (MD) simulations to get an insight into the structure of the complex. AN although not water soluble gave a clear solution in presence of host OA. Under this condition inclusion of AN within OA was confirmed by the changes in the signals of both OA and AN hydrogens in the ^{1}H NMR spectrum.[40]

Host-Guest Complexation–NMR studies: NMR titration spectra resulting from the addition of AN to the host OA in borate buffer are shown in Figure 1. Due to AN's insolubility in water reverse titration by addition of OA to AN could not be carried out. Figure 1(i) and (v) display the signals due to OA and 2:2 complex, respectively. As can be seen, the signals due to both OA and AN are significantly altered in Figure 1(v). Most important is the presence of signals of AN at $\delta \sim 2.95$, 3.5, 5.65, 5.9 and 6.3 ppm (marked in the spectra as # 1-5). Such a remarkable upfield shift from $> \delta$ 7 ppm in $CDCl_3$ to δ between 2.95 and 6.3 in borate buffer due to diamagnetic shielding of the OA cavity is an indication of inclusion of AN within OA.[59-60] The above upfield shifted signals are indeed due to AN hydrogens was confirmed by including perdeuterated AN as the guest. As seen in Figure 1(vi) while the OA signals remained, that due to AN hydrogens were not seen. Upon carefully examining the spectra displayed in Figure 1 (ii) to (v) one can conclude that AN forms a stable 1:1 stoichiometric complex with OA in presence of one equivalent of OA. Further addition of AN does not result in any changes to the spectra displayed in Figure 1(v) suggesting that the complex present in Figure 1(v) does not undergo further changes. However, at early stages of addition wherein excess OA is present with respect to AN, signals due to 1:2 complex (guest to host) are visible. For example, in Figure 1(ii) while the OA signals are significantly altered indicating the complex formation, the five signals due to AN (1:1 complex) are not seen. However, three upfield shifted signals could be identified between δ 4.5 and 7.2 ppm (marked in circles). These we interpret to be due to 1:2 complex (emission spectra discussed later provide a clear evidence in favor of this). In Figure 1(iii), upon further addition of AN to the solution mentioned in Figure 1(ii), in addition to the above indicated three signals, five signals due to 1:1 complex appeared. Addition of more AN to Figure 1(iii) results in spectra shown in Figure 1(v) in which only the five signals due to AN are

present. In this the three signals due to 1:2 complex were replaced by signals due to 1:1 complex. We interpret this series of changes in spectra in Figure 1 to the formation of 1:2 (guest to host) complex at early stages of addition of AN to OA (excess OA with respect to AN) and to its transformation to stable 1:1 complex when the solution contains equal amounts of OA and AN are present. Thus, based on ^{1}H NMR titration spectra we conclude: (a) AN is readily included within OA in borate buffer solution to yield a transparent solution. (b) Addition of AN to OA initially results in 1:2 guest to host complex and depending on the amount of AN present 1:2 and 1:1 complexes exist in equilibrium. (c) Even when more than one equivalent of AN is present 1:1 stoichiometric complex alone is present in solution. A point to note is that 1:1 stoichiometric complex also means 2:2 host-guest complex. We believe, based on emission spectra discussed below the main complex present in solution is 2:2.[40, 59] But 1:1 and 2:2 complexes represent different types of host to guest complex structures. The former is an open cavitandplex while the latter is a fully closed capsuleplex. Structures of various possible complexes are provided as Supporting Information (Figure S1).

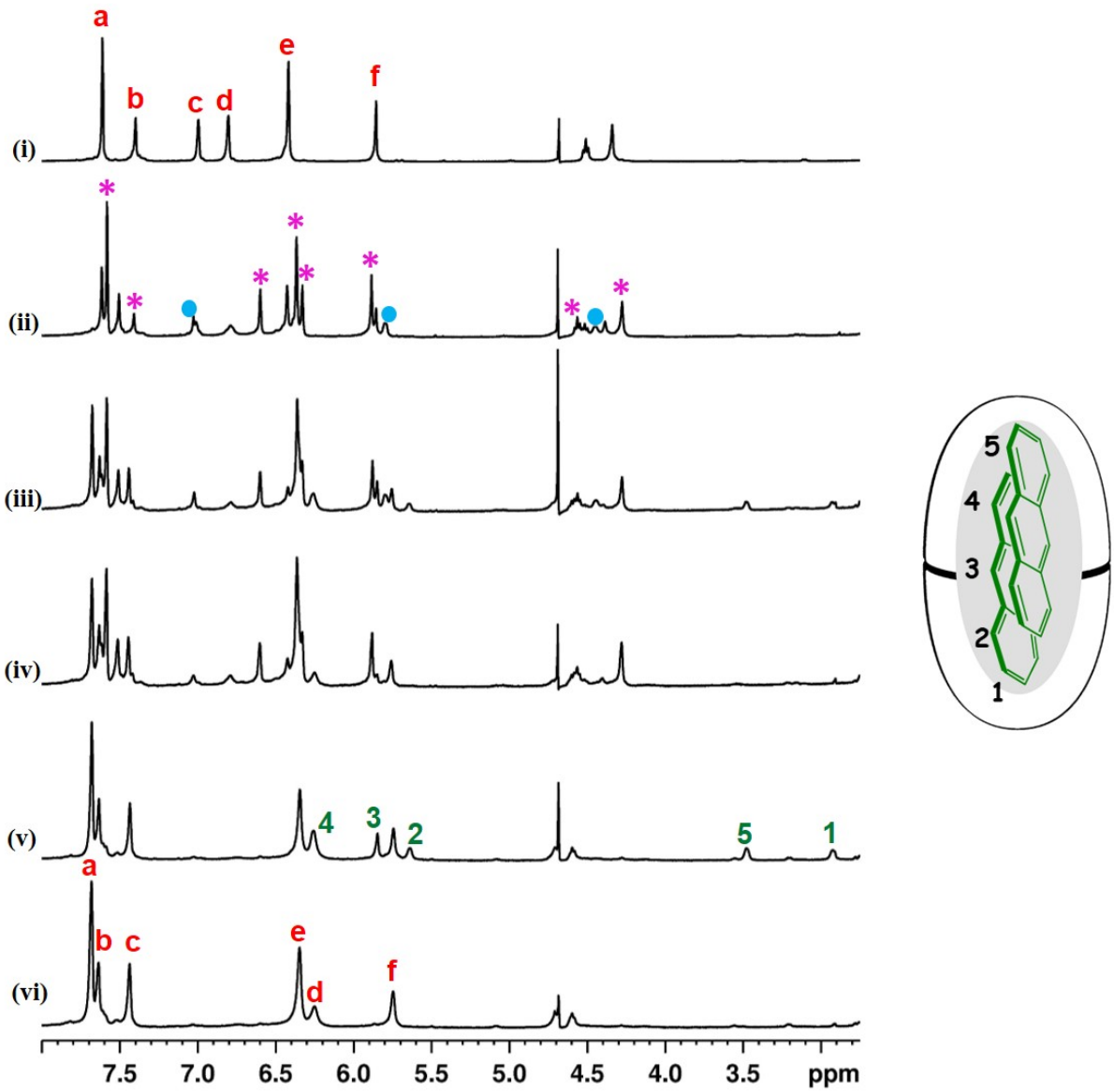

Figure 1. ^{1}H NMR spectra of AN in octa acid. (i) OA (1 mM in 10 mM buffered D_2O), (ii) OA : AN 10:2, (iii) OA : AN 10:6, (iv) OA : AN-d_{10} 10:6, (v) OA : AN 10:10 and (vi) OA : AN-d_{10} 10:10. (**1-5** denotes the AN protons oriented inside OA as 2:2 complex as shown above, red stars denote OA protons of 2:1 complex and blue circles denote the AN protons of 2:1 complex.

Based on the 1:1 stoichiometry inferred from 1-D NMR spectra three different structures for AN@OA complex could be visualized, 1:1 cavitandplex, 2:2 capsuleplex where two AN molecules are placed directly one above the other (symmetrical sandwich structure) and 2:2

capsuleplex where the two AN molecules are placed one above the other but slightly slipped along the long axis (slipped sandwich structure, Figure S1). The cavitandplex where half of the AN framework is exposed to water is eliminated based on peak assignments using COSY spectra. In cavitandplex three upfield shifted signals and two with no shift would be expected. The fact that all five signals are upfield shifted rules out the 1:1 cavitandplex structure. Between the two possible 2:2 capsuleplex structures (symmetrical and slipped sandwich), presence of five signals in NMR favors the slipped one. Symmetrical sandwich structure would give rise to an NMR spectrum with only three signals. Slipped sandwich structure is also consistent with the NOESY correlations.

Host-Guest Complexation–Molecular Modeling: To confirm the proposed structure molecular dynamics (MD) simulations were performed as per the procedure outlined in the experimental section and the results are shown in Figure 2a. Based on NMR spectra and MD simulations we conclude that two molecules of AN are held within OA in a slipped sandwich arrangement. Most likely such an arrangement is favored by π–π stacking between two AN molecules (distance 3.26 Å; Figure 2b). Inclusion of AN within OA is probably facilitated by π–π interaction between AN molecule and aromatic walls of the capsule (3.5 Å) and hydrophobic effect due to aqueous exterior. Perusal of Figure 2a also reveals the lack of free space around the AN molecules. This arrangement hints at the lack of free space around the two AN molecules for any type of reaction. Such a congested arrangement would forbid the photodimerization within the closed capsule. In fact, attempts to include the synthetic dimer dianthracene, the product of photodimerization, within OA were not successful. Another point to note is that the proposed slipped sandwich structure is not the ideal geometry for excimer formation. Formation of excimer as in organic glass or crystal at 77° K would require the two AN molecules to move a total of ~ 1.9 Å along the long axis and closer to attain a symmetrical sandwich arrangement in the excited state.

(a)

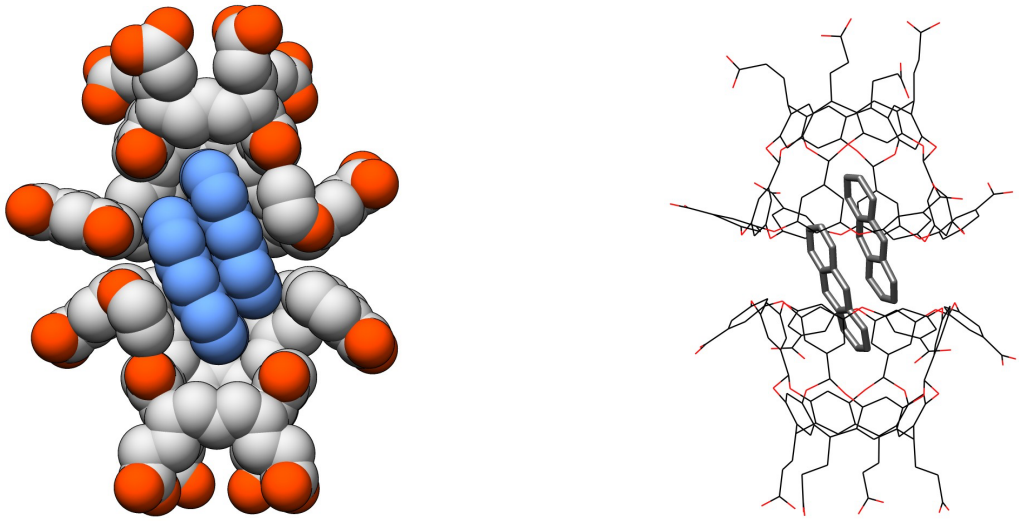

(b)

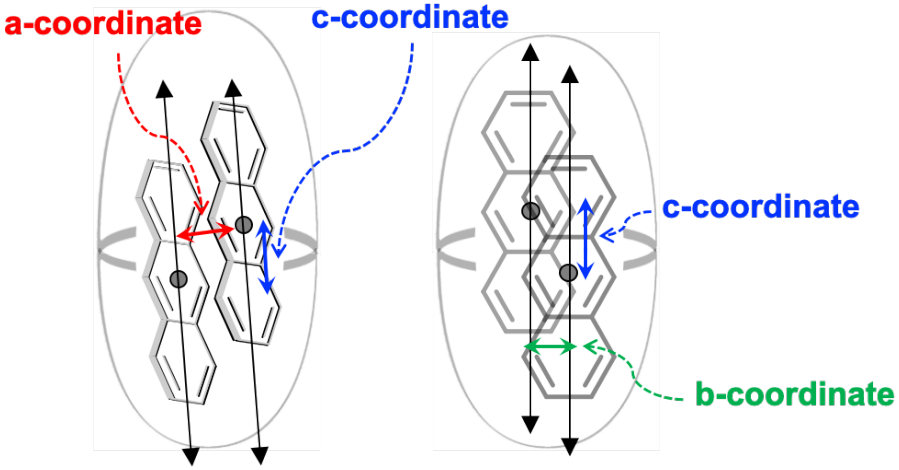

Figure 2. Molecular dynamics (MD) equilibrated structure of the $AN_2@OA_2$ complex in space-filling and wire modes. The distance between two AN within the capsule is 3.26 Å. Distance between AN and OA wall is 3.5 Å. Two AN molecules are slipped along the c axis by 1.9 Å.

Host-guest complexation followed by emission spectroscopy: Having inferred from NMR and molecular dynamics calculations that AN forms 2:2 complex with OA, and having realized that titration by addition of OA to AN in buffer could not be carried out due to solubility problems to unequivocally identify the presence of 1:2 or any other complex by NMR, we performed the titration at much lower concentration and followed the complexation by emission of AN. In Figure 3 the emission spectra of AN upon slow addition of OA (from 0.5 to 50 μM) to a solution of AN (5 μM) in borate buffer are displayed. We believe the initial spectrum resembling that of the monomer is due to AN aggregates. Upon slow addition of OA, the intensity of the above fluorescence decreased while at the same time a broad emission with a maximum at 520 nm appeared and intensified (follow the red spectra in Figure 3a) and reached a maximum at 5 μM (1:1 equivalent). At this stage most emission is broad and resembled the sandwich dimer (excimer) emission at 77 K reported by Chandross and others.[9-11, 17-19, 61-62] Further addition of OA did not lead to total elimination of monomer emission but resulted in decrease of the broad emission and increase of monomer fluorescence (follow the green spectra in Figure 3b). Upon addition of 10 equivalents of OA the excimer emission disappeared leaving only the monomer emission. An immediate question arose, whether the final monomer emission (green in Figure 3b) and the one we started with (black in Figure 3a) are same or different. Close examination of the emission peaks revealed the two are not identical. The excitation spectra of the two were also different (see below for discussion and Figure 4). The observed emission in presence of excess OA is similar to AN emission in benzene (for absorption and emission spectra in solvents see Figures S2–S5). Considering the internal polarity of OA capsule is similar to that of benzene, similarity between the emission within OA and in benzene is not surprising.[60] Apparently when excess OA is present, each AN molecule seeks out a capsule and forms a 1:2 complex. When OA is in short supply a single capsule accommodates two AN molecules. Based on the above titration experiments we believe buffer solutions containing mainly $AN@OA_2$ and $AN_2@OA_2$ could be prepared by controlling the amount of OA in solution. The dependence of the nature of the complex on OA concentration cautions one to avoid using more than an equivalent of OA to observe the AN excimer emission. One of the most important observations relates to the ability to record excimer emission from AN at room temperature in solution.

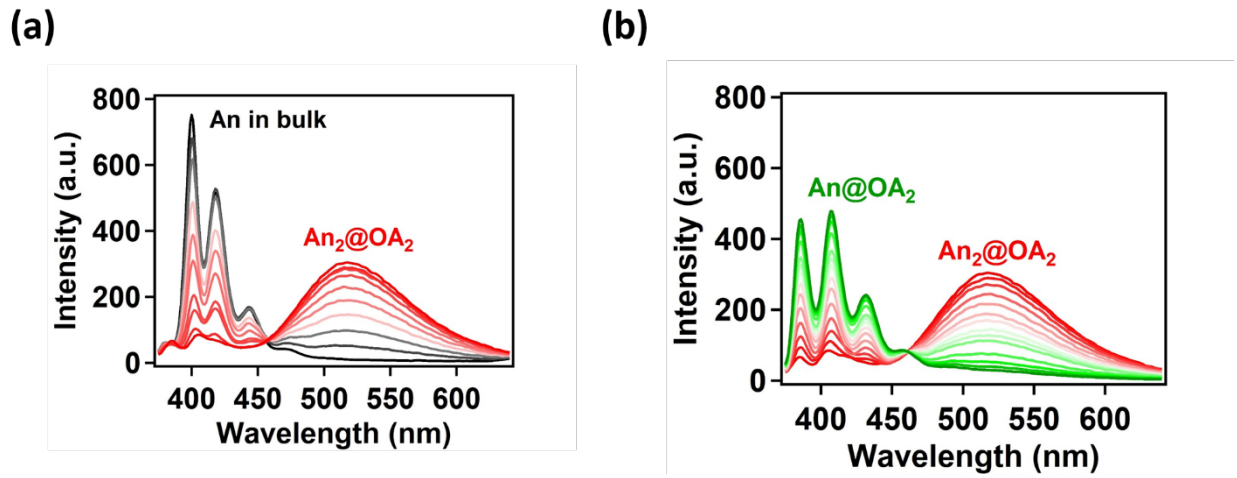

Figure 3. (a) Formation of $AN_2@OA_2$ complex (red) from bulk AN monomer (black) followed by (b) formation of $AN@OA_2$ complex (green) upon addition of excess octa acid. Concentration range: ([An] = 5 x 10^{-6} M ; [OA] = 0 to 5 x 10^{-5} M)

Careful perusal of Figure 3 revealed that the monomer emission of AN could not be completely eliminated at any concentration of OA. Although contribution of the monomer emission could be reduced, it could not be eliminated. This gave rise to an important question: Whether the AN molecule present in 2:2 complex is responsible for the monomer emissions seen in Figure 3? To answer this question two samples that show both monomer and excimer emissions were prepared. Interestingly, a small variation in the OA concentration resulted in change of the nature of the minor emission as seen by its maximum, 420 *vs* 410 nm in Figure 4(a). In Figure 4(b) the excitation spectra for emissions from aggregates as well as from $AN@OA_2$ and $AN_2@OA_2$ complexes are included. Perusal of these reveals that the excimer excitation spectrum is distinctly different from those of the emissions from 1:2 complex and AN in water. Also, none of the excitation spectra of the monomer emissions resemble that of the excimer. This rules out the possibility that capsules containing two molecules of AN being responsible for the monomer emissions with either 410 or 420 nm maxima. Further they suggest that excitation of $AN_2@OA_2$ capsules results mainly in excimer emission. For expanded absorption, excitation and emission spectra of $AN@OA_2$ and $AN_2@OA_2$ complexes see Figures S6–S12 in supporting information.

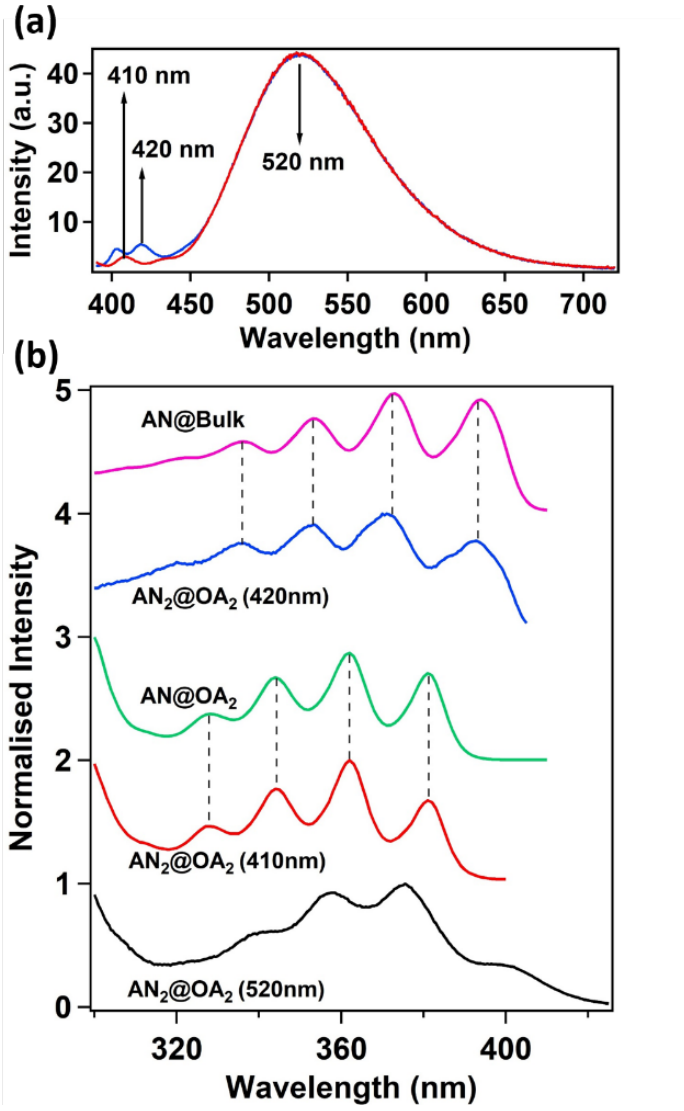

Figure 4. (a) Emission spectra of AN incubated in OA when AN:OA is slightly less than 1:1 (blue solid line) and AN:OA is slightly greater than 1:1 (red solid line). (b) Comparison of the excitation spectra of free AN in bulk, AN@OA_2, monomeric and excimer emission for samples described in a.

Having established a procedure to generate AN excimer in solution at room temperature we were curious to compare its lifetime with the early reports that claimed to have recoded the excimer emission in solution at room temperature. Fluorescence transients of AN in

cyclohexane, AN@OA_2 and AN_2@OA_2 are shown in Figure S13. Lifetimes extracted from these decays are tabulated in Table 1. The long lifetime of 235 ns for emission with 520 nm maximum is closer to the values reported for sandwich dimers at 77 K (>200 ns)[12, 14-15, 20] and far away from the value reported for very weakly emissive excimer in solution at room temperature (<2 ns).[33-35] The long lifetime suggests that the excimer experiences significant constraint within the capsule as in crystals and glassy matrix at 77 K.

Table 1. The average lifetime of anthracene in bulk and in 1:2 & 2:2 complexes in aqueous buffer medium.

Species	**Wavelength (nm)**	τ_{avg} **(ns)**
AN in cyclohexane	410	4.0
AN@OA_2	410	3.6
AN_2@OA_2	410	5.9
	520	235

Time-resolved emission experiments: Usually the excimer formation in isotropic solution medium is controlled by diffusion. In this respect, our system is quite unique like the sandwich dimer pre-prepared in crystals and organic glass at 77 K. Two monomers of AN being held together in close proximity inside the OA cavity nullifies the need for the two molecules to diffuse towards each other. This arrangement is ideal to investigate the dynamics of excimer formation excluding the first step of diffusion. Based on the structure shown in Figure 2a we realized that at least two distinct motions are required to attain the favorable geometry for excimer formation. The two AN molecules must move closer (a-axis in Figure 2b) and slip along both b and c-axes to be fully on top of each other to attain total π–π overlap. Time-resolved experiments were performed to gain insight into the nature of movements the AN*–AN pair within the confined space of OA to reach the above geometry.

We recorded time-resolved emission throughout the whole range of the broad band emission of $AN_2@OA_2$. Presence of a delay in the excimer emission build up (Figure 5a) confirms that only one of the two AN is excited and it reaches out for another ground state AN to form the excimer. This is also consistent with the excitation spectrum of the excimer (Figure 4), which has most of the features of the monomer absorption. As seen in Figure 5b, immediately upon excitation only monomer type emission dominates (violet and greenish blue lines) and with time excimer emission builds up. This is consistent with the conventional monomer-excimer buildup often displayed in textbooks. The most unusual feature of the time resolved spectra shown in Figure 5b is the maximum of broad excimer emission shifting with time. Such a behavior is not known in solution during excimer formation of any aromatic molecules. This we believe is an indication of the difference in excited state surface connecting monomer to excimer within a confined space and isotropic solution. To examine this further we analyzed mainly the excimer emission. The 400-420 nm region has been excluded from the analysis as contribution for this emission also comes from 1:2 complex (Figure 4 and Figure S12). Construction of time-resolved emission spectra (TRES) reveals gradual shift of emission spectra from 458 nm to 520 nm with time (Figure 5c). One important point to note is that the time zero spectra (458 nm) is much red shifted and broad compared to the monomeric emission in bulk and 1:2 complex (410 nm maximum). The broadness suggests that the emission must involve two molecules interacting with one another. If it is due to a single molecule one would expect it to be structured. Perhaps the very short distance between the two monomers trapped inside the cage is the reason behind this observation. Appearance of excimers with different emission maxima suggests that excited state surface must not be steep, and the motion must be slow. Apparently, the radiative transition is able to compete with forward motion towards the stable excimer structure. Surprisingly the peak frequency *vs* time plot (Figure 5d) reveals that the shift of emission is not monotonous. This unusual behavior of variation of peak frequency with time suggests that the total relaxation process may involve multiple steps.

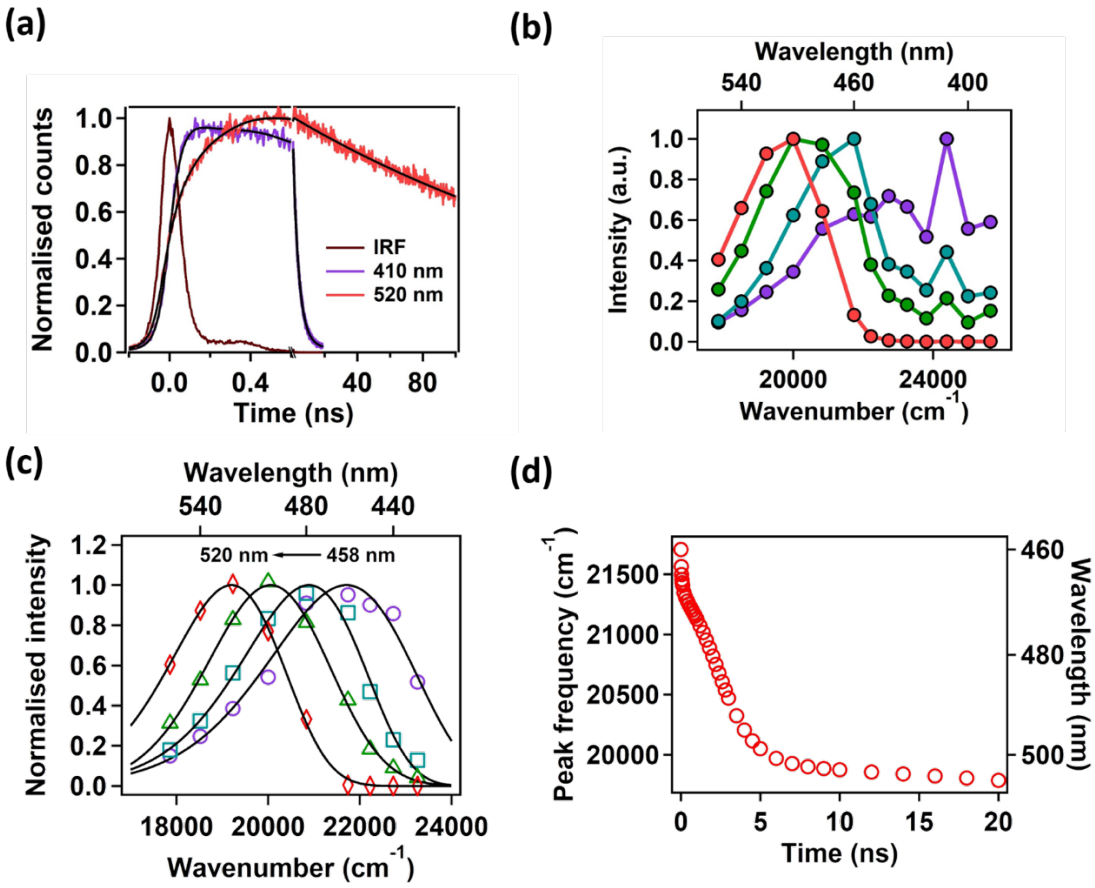

Figure 5. (a) Fluorescence transients of $AN_2@OA_2$ complex upon exciting at 375 nm. Multiexponential fitted lines to the transients are displayed in black. Note: the fluorescence transient at 520 nm has a rise component. (b) Representative time resolved emission spectra, TRES, (purple: 0 ns; cyan: 0.5 ns; green: 3 ns; red: 20 ns) constructed from the fitting parameters of fluorescent transients at different wavelength along the steady state emission spectra (390-560 nm). (c) Some representative TRES in the excimer region (purple circles: 0 ns; cyan squares: 1.8 ns; green triangles: 5 ns; red diamonds: 70 ns) fitted to lognormal function (solid black lines). In this case we have excluded the wavelength region 390-420 nm which is mainly contributed by AN@OA2 and free AN in bulk. (d) Variation of emission peak-frequency with time.

To probe this likelihood, time-resolved area normalized emission spectra (TRANES) were generated (Figure 6).[63-65] Two isoemissive points could be identified in the TRANES at two different wavelengths at two different time window (see Figures 6a and c). This is a clear

indication of a two-step process involving three states. From t = 0 to 0.1 ns, the first isoemissive point appeared at 448 nm. The second isoemissive point at 487 nm is observed in the t = 0.3 ns to 16 ns time window. In order to determine the rate constant of the first step we plotted the ratio of the intensity of the peak at t = 0 ns to the intensity of the peak at t = 0.1 ns with time. From its exponential fitting we found the rate constant of the first step to be 17.40 ns^{-1} (Figure 6b). A similar approach was taken to determine the rate constant of the second step. Exponential fit to the intensity ratio against time plot gave the rate constant as 0.377 ns^{-1} (Figure 7d), which is indeed a much slower process compared to step 1. Based on the above observations a model shown in Figure 7 is proposed. In this model, AN* soon after it is formed interacts with the close-by AN and both molecules together start their journey from 'M' to 'O' via 'N'. A possible barrier from 'N' to 'O' is indicated in the Figure. In conclusion, encapsulation of two monomeric AN inside OA cavity nullifies the effect of diffusion in the excimer formation dynamics which enables us to look into the molecular dynamics prior to the excimer formation. We have found that the process of excimer formation is a two-step one. The first step being a barrierless one is a much faster with rate constant 17.4 ns^{-1}. Whereas the second step has a potential barrier hand hence a much slower step with rate constant 0.377 ns^{-1}.

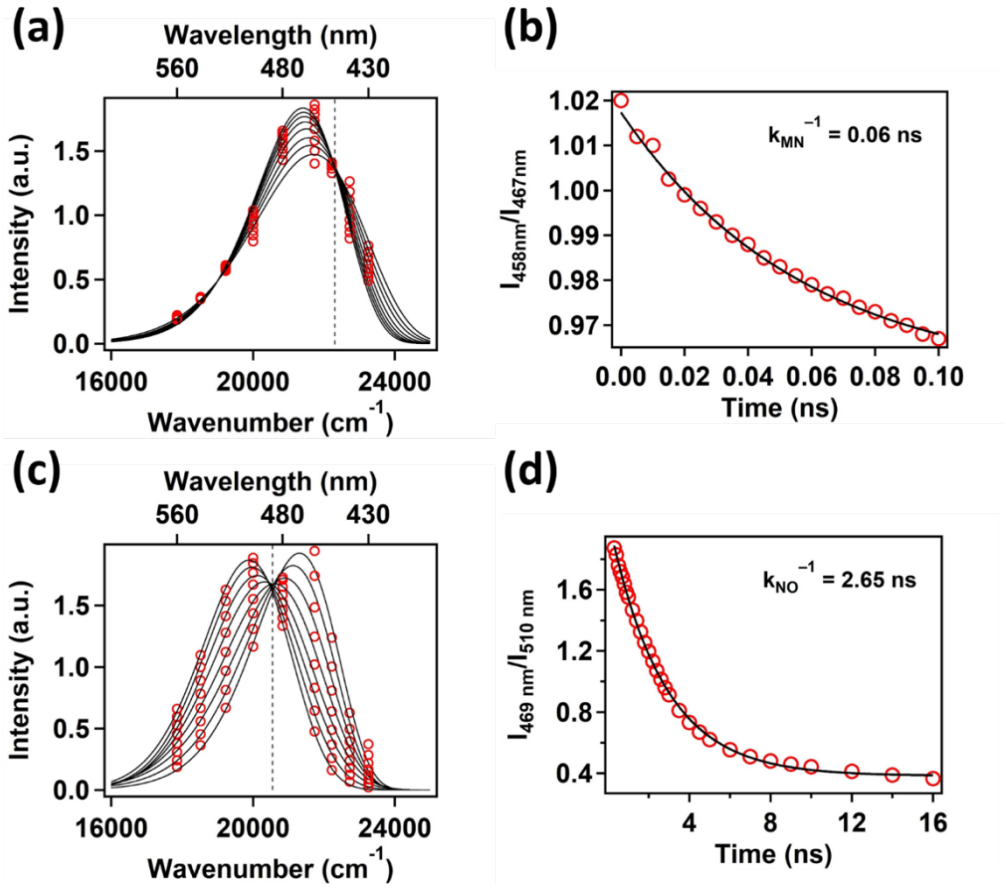

Figure 6. (a and c) TRANES showing the isoemissive point at different wavenumber at different time. Two different isoemissive point indicates the overall process of energy relaxation occurs through two different steps. (b and d) Time evolution of the ratio of the intensity of the initial state and the final state for each of these two steps. They were fitted exponentially. Fitted line is given in black.

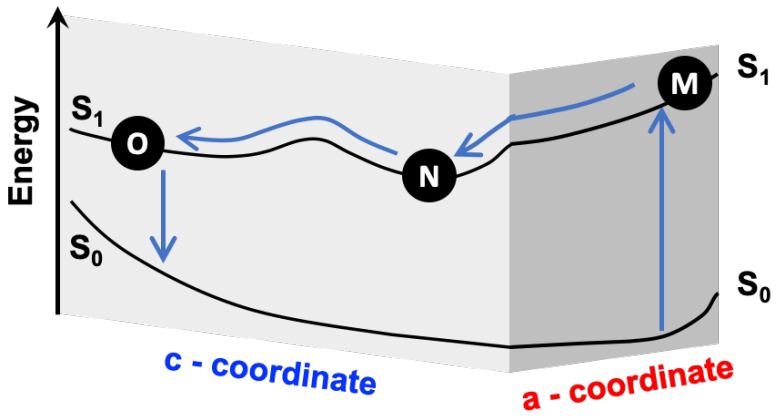

Figure 7. Kinetic model based on the result of TRES and the theoretically calculated PES.

To check the presence of energy barrier as per the model shown in Figure 7, we recorded emission spectra of $AN_2@OA_2$ from 278 to 343 K. The excimer emission gradually decreased with increase in temperature (see SI for details). This is not consistent with the above model. Furthermore, in solution, where the monomer–excimer equilibrium is established, the temperature dependence of excimer shows a bimodal dependence.[66-69] In one region the excimer emission increases and in the other it deceases with temperature. In this study, the stability of $AN_2@OA_2$ also depends on the temperature. Thus, we realized that temperature dependent excimer emission would not be useful in verifying the model. This prompted us to obtain an insight into the temperature effect on excimer formation by quantum chemical calculations. By this approach we mapped out the excited state surface connecting monomer and excimer results which are discussed in the next section.

The above model as well as the delay in the excimer emission (Figure 5a) suggest that AN* has a transient existence before interacting with the adjacent ground state AN. If this is true it should be possible to quench it with an external quencher such as MV^{2+} before the start of the excimer emission. In Figure 8(c) steady state emission spectra of AN in 2:2 complex in presence of methylviologen^{2+} (MV^{2+}) are displayed. Weak monomer and strong excimer emissions are seen. Upon incremental addition of MV^{2+} the intensities of both emissions (410

nm and 520 nm) decreased indicating quenching by MV^{2+} (see Figure 8(c)). On the other hand, decay of the monomer and excimer emissions are not significantly influenced by MV^{2+} (Figure 8(a) & (b)). The Stern-Volmer plots shown in Figure 8(d) suggest that the quenching is static in origin. In order to probe the origin of the quenching we recorded the transient absorption spectra of the $AN@OA_2$ and $AN_2@OA_2$ separately following the addition of MV^{2+}. In the TA spectra for both the cases (Figure 9(a) & (c)), we observe a positive signal developing around 615 nm, which is a well-known indication of the formation of methyl viologen radical cation ($MV^{\bullet+}$) as a product of photoinduced electron transfer (PET) reaction.[41] Time constant of formation of $MV^{\bullet+}$ is the rise component obtained from fitting of the kinetics at 615 nm and gives the actual rate constant of PET. These rate constants of PET for $AN@OA_2$ and $AN_2@OA_2$ are measured as 0.196 and 0.187 ps^{-1}, respectively, which are nearly the same. The high rate constant reported here is consistent with our recent studies on electron transfer between OA encapsulated aromatics and viologens present outside the capsule.[70] In the case of $AN_2@OA_2$, the much higher rate constant of PET compared to that one associated with the excimer formation dynamics stated earlier (2.65 ns) suggests that electron transfer takes place at the very early stages of the excimer formation process and the two AN do not get the chance to relax to the most stable excimeric conformation before the quenching process. To our knowledge this has not been recognized previously. The similarity in the rate constants of PET for $AN@OA_2$ and $AN_2@OA_2$ also suggests that at the time scale as small as ~5 ps it is possible that the emission from the FC state of $AN_2@OA_2$ may have much more similarity to the monomeric emission of $AN@OA_2$ than we estimated from the time-resolved studies in the earlier sections as time-resolved studies at ps-resolution is beyond the scope of our experimentation in case of such a slow process like excmier formation.

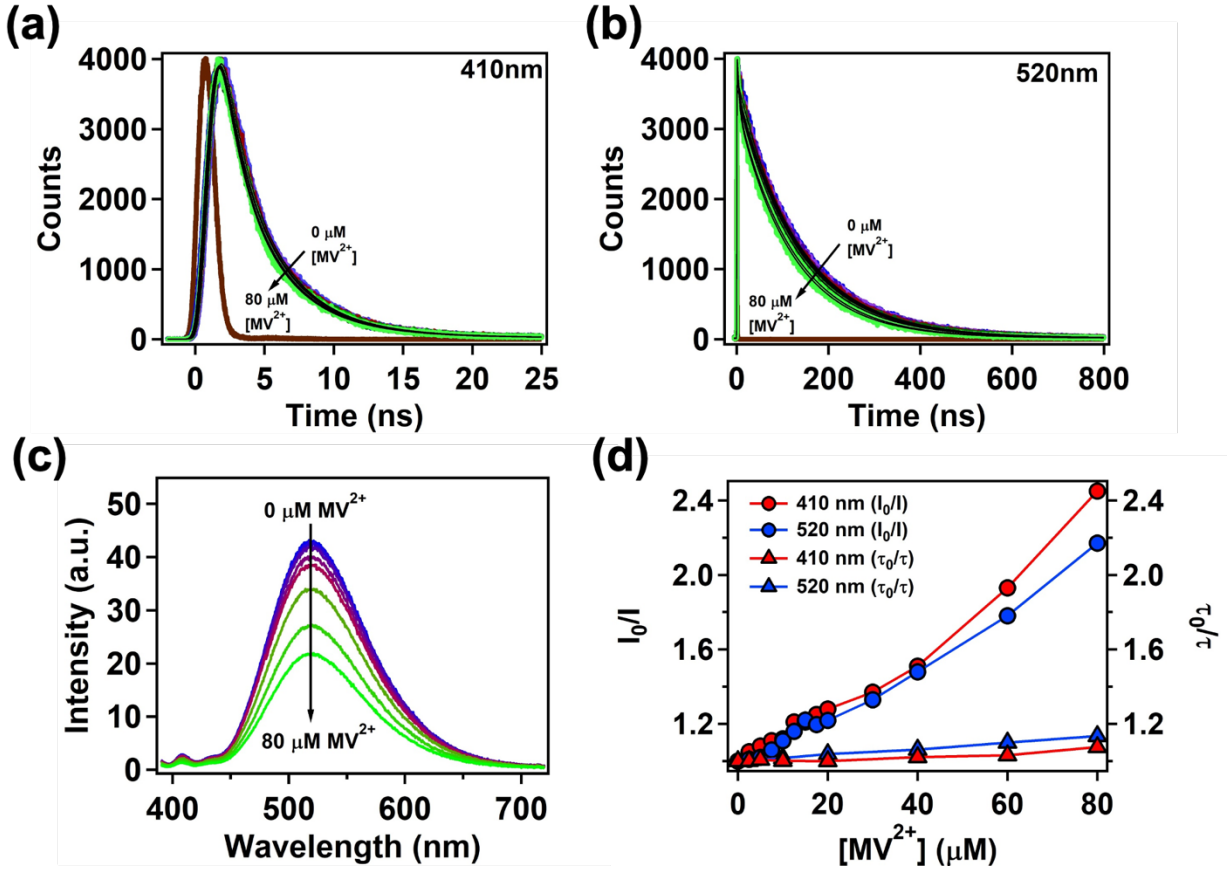

Figure 8. (a) Fluorescence transients recorded at (a) 410 nm, (b) 520 nm and (c) steady state fluorescence spectra of $An_2@OA_2$ recorded with increasing concentration of MV^{2+}. (d) Stern-Volmer quenching plot between $An_2@OA_2$ and MV^{2+}. ([AN] = 25 μM and $[MV^{2+}]$ = 0 – 80 μM)

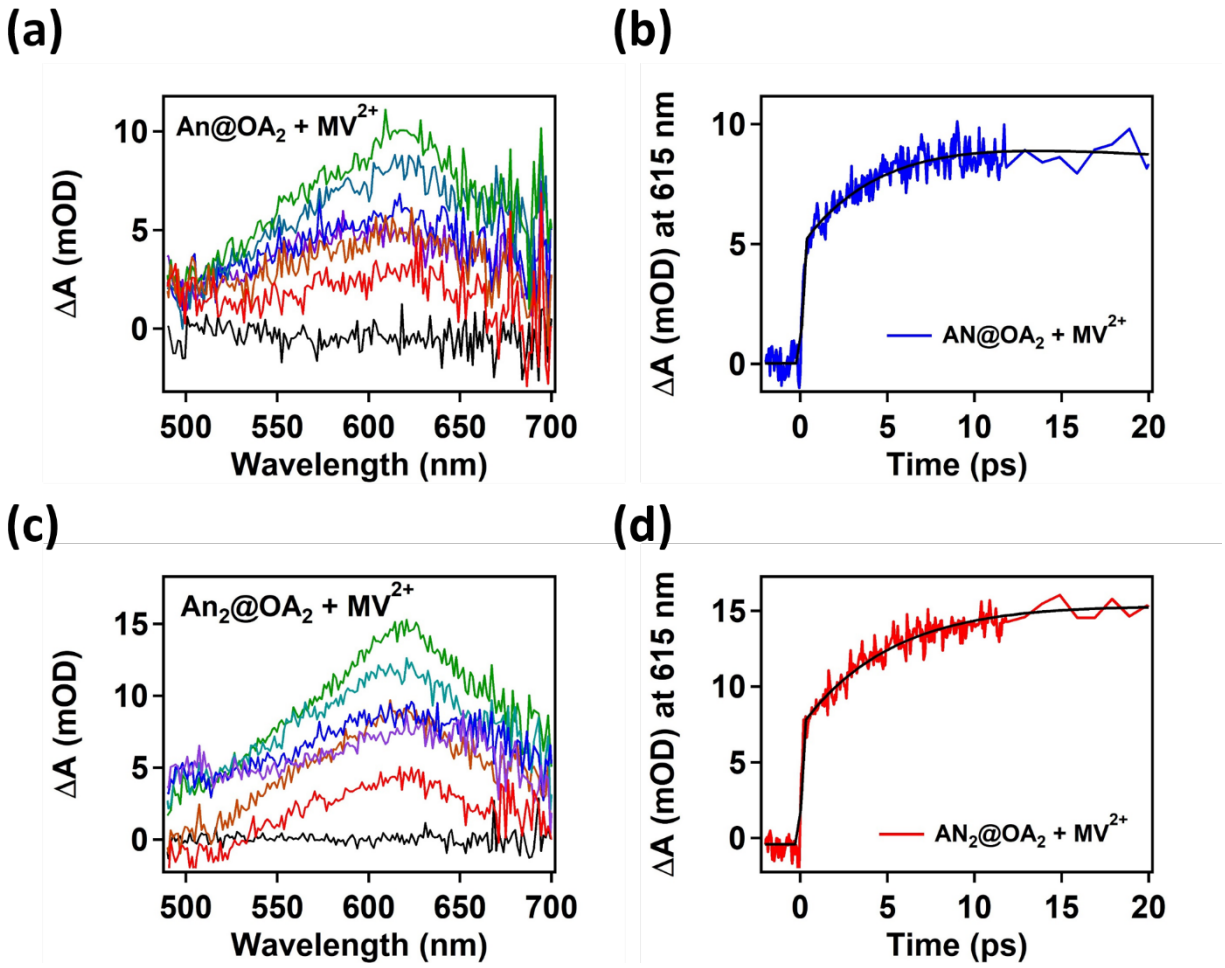

Figure 9. Transient absorption spectra (a & c) at some selected time delays (black: 0 ps; purple: 0.5 ps; blue: 1 ps; cyan: 5 ps; green: 20 ps; orange: 400 ps; red: 1000 ps) and fitted kinetics at 615 nm (b & d) for AN@OA_2 and AN_2@OA_2, respectively, in presence of MV^{2+}. ([AN] = 100 μM and [MV^{2+}] = 10 mM)

Quantum mechanical model for excited state dynamics: The DFT optimized ground state (S_0) structure of the complex is similar to the equilibrated structure obtained in the MD simulations (see Figure 2). The two AN molecules are in a slip-stacked configuration with a distance a= 3.544 Å between their parallel planes and having relative displacements of b=1.003 Å and c=2.089 Å along the short and long axes, respectively. The molecules are oriented at 18 degrees to the axis of the OA cavity. Compared to the gas phase optimized structure (see Table

S1), the confined dimer is significantly more slipped along *c*. In order to understand the mechanism of excimer formation, we explored the ground and excited potential energy curves (PEC) of the two AN molecules in the OA cavity along the *a*, *b* and *c* coordinates (see Figure 2(b) for axis notations). In particular, the first three singlet excited states (S_1, S_2 and S_3) were tracked in the PEC along with the ground state (S_0). The results are plotted in Figure 10. Unlike in the gas phase (see Figure S15), the PECs for the slip displacements (*b* and *c*) in the confined AN dimer are unsymmetrical about the sandwich-like arrangement. The S_1 PEC along *c* exhibits a minimum at 2.33 Å (Δc = 0.19 Å in Figure 10 (a)) corresponding to a naphthalene-like (NL) excimer,[71] where the molecules are π -π stacked through only two of three benzene rings from each AN. Instead, the anthracene-like (AL) excimer with all three rings π -π stacked is not stable in the OA cage, although it is the deeper minimum in the gas-phase (see Figure S15). Inside the cage, a minimum corresponding to the AL excimer appears on S_1 around Δc = -1.43 Å (i.e. *c*=0.66 Å) but is higher in energy by 0.18 eV than the NL excimer (see Figure S16).

Throughout most of the PEC S_2 has a much higher oscillator strength than S_1, though both have nearly similar energies, especially in the Franck-Condon region. Therefore, the absorption at 376 nm seen in experiments, is most likely due to an excitation to S_2. The theoretically predicted excitation energy to S_2 of 363 nm in good agreement with the experiment. An estimate of the gradients along the three coordinates considered indicates that the motion on the S_2 surface will be predominantly along *a* and *c* coordinates. This is also evident from the PEC plots in Figure 10. The PEC along *c* features an avoided crossing between S_1 and S_2 (S_1/S_2), appearing at $\Delta c \approx$ -0.65 Å, signaling the possibility of surface crossing during dynamics in the excited state. Therefore, we propose that after the vertical excitation to S_2, the system will be driven, along both *a* and *c* axes, towards the S_1/S_2 region where it will most likely cross to S_1 and be stabilized as the NL excimer. Excimer emission wavelengths can be estimated by computing the S_0 to S_1 vertical energies at a geometry with the minimized *a*, *b* and *c* distances extracted from the PEC. Since the S_1 energy does not change much about the minimized *b* value (0.47 Å) we assumed that *b*=0 Å in the excimer geometry. PEC along *a* and *c* were recomputed with this constraint to extract the relevant minima. The minimum along *a* occurs at 3.38 Å while there are two minima along *c* located at *c*=2.35 Å and *c*=0.66 Å corresponding to the NL and AL excimers, respectively (see Figure S16). From these we estimate an emission wavelength of

490.8 nm for the NL excimer and 539.1 nm for the AL excimer. It is possible that the AL excimer slowly converts to the NL excimer, over a barrier of 0.19 eV, subsequently resulting in the experimentally observed broad fluorescence centered at 520 nm.

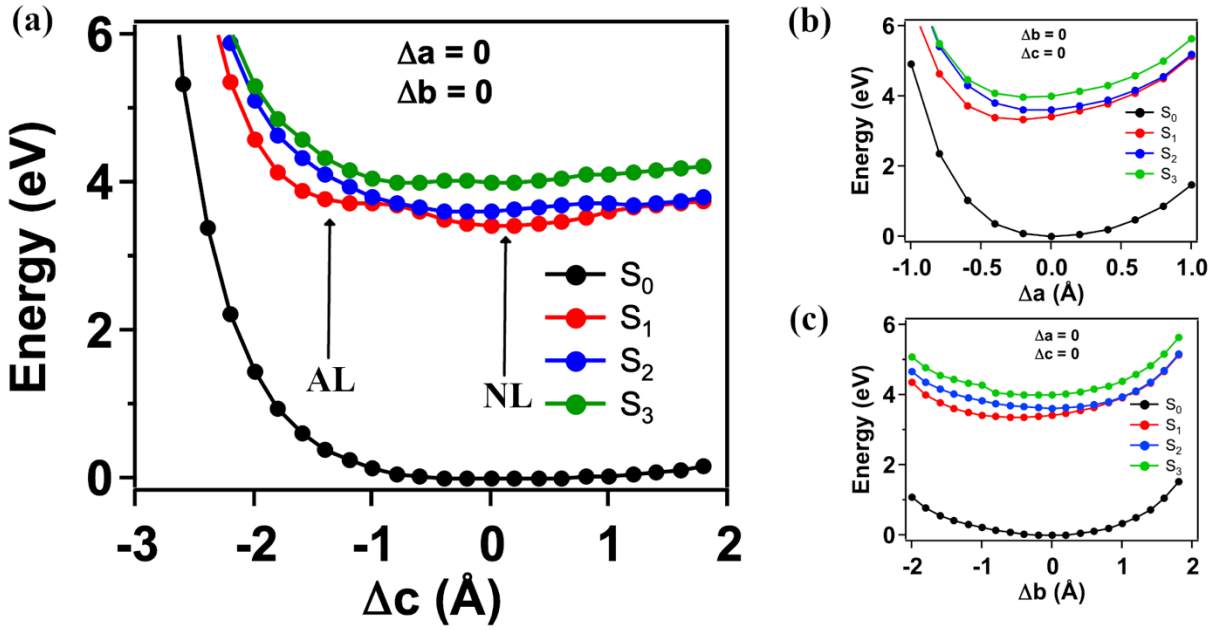

Figure 10. Potential energy curves for the confined anthracene dimer depicting the complex binding energies as a function of the displacement along (a) the *c*-coordinate (long axis) with the locations of the anthracene-like (AL) and naphthalene-like (NL) excimer minima marked, (b) the *a*-coordinate (inter-planar separation), and (c) the *b*-coordinate (short axis). A description of these directions is giving in Figure 2(b). The energies and the displacements are plotted relative to their respective values in the optimized structure (*a*= 3.544 Å, *b*=1.003 Å and *c*=2.089 Å).

Conclusions

Although numerous substituted anthracenes are well-established to show excimer emission, the parent unsubstituted anthracene generally do not show excimer emission in solution. In the 60's considerable effort was spent on understanding this anomalous behavior

resulting in the development of an ingenious method involving photolytic decomposition of dianthracene in organic glass at 77° K. This approach enabled excimer emission from AN to be recorded at 77° K. However, recording excimer emission from AN at room temperature in solution continues to be challenging even now. In this report we have outlined a method that allows recording intense emission from AN excimer at room temperature in aqueous solution. The confined environment provided by a synthetic organic capsule (OA) enhances the photophysical pathway (excimer emission) at the expense of photochemical reaction pathway, namely dimerization. The simple elegant strategy outlined here should be a valuable tool to record excimer emission from reluctant guest molecules.

Host-guest complexation as followed by NMR experiments suggested that AN forms two types of OA complexes, 1:2 and 2:2 (guest to host). The ratio of these complexes could be controlled by careful manipulation of the relative concentrations of OA and AN in solution. Excitation and absorption spectra of monomer and excimer emissions reveal that the AN molecule present in 2:2 complex shows mainly excimer emission. One of the novel observations relates to the time dependent emission maxima of the excimer. In solution, excimer emission has a single maximum indicating the monomer to excimer in the excited surface is a steep descent. Interestingly, time resolved emission studies has uncovered a unique feature thus far unknown with respect to excimer emission in solution. The time dependent AN excimer emission maxima suggest that the potential energy surface leading from excited monomer to excimer is not steep and the pathway within the OA capsule is tortuous. Time-resolved area normalized emission spectra reveal the path to be bumpy with at least two peaks in between. Computational and quantum chemical calculations suggest that due to the restricted space within OA capsule the two AN molecules are not ideally placed in the ground state for excimer formation. The calculated potential energy curves are consistent with the experimental observations. The results presented here supports the conclusion that molecules when confined behave differently.[70, 72-74]

AUTHOR INFORMATION

E-mail: psen@iitk.ac.in

E-mail: murthy1@miami.edu

E-mail: vardha@iiserb.ac.in

E-mail: rpr@miami.edu

ORCID

Pratik Sen: 0000-0002-8202-1854

Vaidhyanathan Ramamurthy: 0000-0002-3168-2185

Varadharajan Srinivasan: 0000-0001-9666-8985

Rajeev Prabhakar: 0000-0003-1137-1272

Notes

The authors declare no competing financial interest.

Supporting Information

The Supporting Information is available free of charge at https://pubs.acs.org/doi/10.1021

Cartoon representation of various types of complexes, absorption, emission and excitation spectra of anthracene monomer and excimer, structural parameters from DFT optimizations

ACKNOWLEDGMENTS

V.R. and R.P. thank the National Science Foundation (CHE-1807729 and CHE-1664926) for financial support. P. S. thank Indian Institute of Technology Kanpur for infrastructure and financial support. A.D. acknowledges Ministry of Electronics & Information Technology (MeitY), Government of India for providing fellowship under the Visvesvaraya PhD scheme. S.B. and V.S. thank IISER Bhopal for providing High Performance Computing facilities and funding. The support and the resources provided by Centre for Develoment of Advanced Computing (C-DAC) and the National Supercomputing Mission (NSM), Government of India are gratefully acknowledged.

References

1. Bouas-Laurent, H.; Castellan, A.; Desvergne, J.-P.; Lapouyade, R., Photodimerization of Anthracenes in Fluid Solution: Structural Aspects. *Chem. Soc. Rev.* **2000**, *29*, 43-55.
2. Bouas-Laurent, H.; Castellan, A.; Desvergne, J.-P.; Lapouyade, R., Photodimerization of Anthracenes in Fluid Solutions: (Part 2) Mechanistic Aspects of the Photocycloaddition and of the Photochemical and Thermal Cleavage. *Chem. Soc. Rev.,* **2001**, *30*, 248-263.
3. Birks, J. B., *Photophysics of Aromatic Molecules*; Wiley-Interscience: London, 1970.
4. Bowen, E. J., The Photochemistry of Aromatic Hydrocarbon Solutions. In *Advances in Photochemistry*, W.A. Noyes, J.; Hammond, G. S.; J.N. Pitts, J., Eds. John Wiley & Sons, Inc.: New York, 1963; Vol. 1, pp 23-42.
5. Turro, N. J.; Ramamurthy, V.; Scaiano, J. C., *Modern Molecular Photochemistry of Organic Molecules*; University Science Books: Sausalito, CA, 2010.
6. Forster, T., Excimers. *Angew. Chem. Intnat. Edit.* **1969**, *8*, 333-343.
7. Stevens, B., Photoassociation in Aromatic Molecules. In *Advances in Photochemistry*, Pitts, J. N.; Hammond, G. S.; Noyes, W. A., Eds. Wiley-Interscience: New York, 1971; Vol. 8, pp 161-226.
8. Birks, J. B.; Dyson, D. J.; Munro, I. H.; Flowers, B. H., Excimer Fluorescence Ii. Lifetime Studies of Pyrene Solutions *Proc. R. Soc. Lond. A* **1963**, *275*, 575–588.
9. Chandross, E. A., Photolytic Dissociation of Dianthracene. *J. Chem. Phys.* **1965**, *43*, 4175-4176.
10. Chandross, E. A.; Ferguson, J., Absorption and Fluorescence of Sandwich Dimers. Theory of the Excimer State. *J. Chem. Phys.* **1966**, *45*, 397-398.
11. Chandross, E. A.; Ferguson, J., Absorption and Excimer Fluorescence Spectra of Sandwich Dimers of Substituted Anthracenes. *J. Chem. Phys.* **1966**, *45*, 3554-3564.
12. Fielding, P. E.; Jarnagin, R. C., ``Excimer'' and ``Defect'' Structure for Anthracene and Some Derivatives in Crystals, Thin Films, and Other Rigid Matrices. *J. Chem. Phys.* **1967**, *47*, 247-252.

13. Ferguson, J.; Mau, A. W. H.; Morris, J., Spectra of Dimers of Anthracene and Its Derivatives. Ii. Stable Dimers. *Aust. J. Chem.* **1973**, *26*, 103-110.

14. Mataga, N.; Torishashi, Y.; Ota, Y., Studies on the Fluorescence Decay Times of Anthracene and Perylene Excimers in Rigid Matrices at Low Temperatures in Relation to the Structures of Excimers. *Chem. Phys. Lett.* **1967**, *1*, 385-387.

15. Subudhi, P. C.; Kanamaru, N.; Lim, E. C., Luminescence from a Sandwich Dimer of Anthracene. *Chem. Phys. Lett.* **1975**, *32*, 503-507.

16. Ferguson, J., Excited Dimer (Excimer) Luminescence from Aromatic Molecules in Crystalline Cyclohexane. *J. Chem. Phys.* **1965**, *43*, 306-307.

17. Chandross, E. A.; Ferguson, J., Photodimerization of Crystalline Anthracene. The Photolytic Dissociation of Crystalline Dianthracene. *J. Chem. Phys.* **1966**, *45*, 3564-3567.

18. Chandross, E. A.; Ferguson, J.; McRae, E. G., Absorption and Emission Spectra of Anthracene Dimers. *J. Chem. Phys.* **1966**, *45*, 3546-3553.

19. Ferguson, J., Absorption Spectroscopy of Sandwich Dimers and Cyclophanes. *Chem. Rev.* **1986**, *86*, 957-982.

20. Ferguson, J.; Mau, A. W. H., A Spectroscopic Study of the Photodimerization of Anthracene Sandwich Dimers in Dianthracene. *Molecular Physics* **1974**, *27*, 377-387.

21. Ramamurthy, V.; Weiss, R. G.; Hammond, G. S., *A Model for the Influence of Organized Media on Photochemical Reactions*. John Wiley & Sons, Inc.: 1993; Vol. 18, p 67-234.

22. Weiss, R. G.; Ramamurthy, V.; Hammond, G. S., Photochemistry in Organized and Confining Media: A Model. *Acc. Chem. Res.* **1993**, *26*, 530-536.

23. Forster, T.; Selinger, B., Conccentration Change of the Fluorescence of Aromatic Hydrocarbons in Micellar Colloidal Solution. *Zeitshrift fuer Naturforschung* **1964**, 38-41.

24. Turro, N. J.; Kuo, P.-L., Pyrene Excimer Formation in Micelles of Nonionic Detergents and of Wwater-Soluble Polymers. *Langmuir* **1986**, *2*, 438-442.

25. Patonay, G.; Shapira, A.; Diamond, P.; Warner, M., I., A Systemetic Study of Pyrene Inclusion Complexes with Alfa-, Bita-, and Gama-Cyclodextrins. *J. Phys. Chem.* **1986**, *90*, 1963-1966.

26. Dyck, A. S. M.; Kisiel, U.; Bohne, C., Dynamics for the Assembly of Pyrene-G-Cyclodextrin Host-Guest Complexes. *J. Phys. Chem. B* **2003**, *107*, 11652-11659.

27. Cheng, K. A. W. Y.; Schepp, N. P.; Cozens, F. L., Ultrafast Dynamics of Pyrene Excimer Formation in Y Zeolites. *J. Phys. Chem. A* **2004**, *108*, 7132-7134.

28. Hashimoto, S., Observation of Charge-Resonance Band of Naphthalene Dimer Cation Confined in Cavities of Faujasite Zeolites. Near-Ir Diffuse Reflectance Laser Photolysis Study. *Chemical Physics Letters* **1996**, *262*, 292-297.

29. Hashimoto, S.; Fukazawa, N.; Fukumura, H.; Masuhara, H., Observation and Characterization of Excimer Emission from Anthracene Included in Nax Zeolite. *Chem. Phys. Lett.* **1994**, *219*, 445-451.

30. Hashimoto, S.; Ikuta, S.; Asahi, T.; Masuhara, H., Fluorescence Spectroscopic Studies of Anthracene Adsorbed into Zeolites: From the Detection of Cation−Π Interaction to the Observation of Dimers and Crystals. *Langmuir* **1998**, *14*, 4284-4291.

31. Liu, X.; Iu, K. K.; Thomas, J. K., Photophysical Properties of Pyrene in Zeolites. In *J. Phys. Chem.*, 1989; Vol. 93, pp 4120-4128.

32. Moore, G. F., Delayed Excimer Emission from Anthracene. *Nature* **1966**, *212*, 1452-1453.

33. Rodgers, M. A. J., Observation of the Anthracene Excimer During Nanosecond Pulse Radiolysis of Benzene Solutions. *Chem. Phys. Lett.* **1972**, *12*, 612-614.

34. Cohen, M. D.; Ludmer, A.; Yakhot, V., The Excimer as Intermediate in the Photodimerization of Anthracene in Fluid Solution. *Chem. Phys. Lett.* **1976**, *38*, 398-400.

35. McVey, J. K.; Shold, D. M.; Yang, N. C., Direct Observation and Characterization of Anthracene Excimer in Solution. *J. Chem. Phys.,* **1976**, *65*, 3375-3376.

36. Kobayashi, T.; Nagakura, S.; Szwarc, M., Direct Observation of Excimer Formation in Anthracene and 9,9'-Bianthryl. *Chem. Phys.* **1979**, *39*, 105-110.

37. Horiguchi, R.; Iwasaki, N.; Maruyama, Y., Time-Resolved and Temperature -Dependent Fluorescence Spectra of Anthracene and Pyrene in Crystalline and Liquid States. *J. Pjys. Chem.* **1987**, *91*, 5135-5139.

38. Gibb, C. L. D.; Gibb, B. C., Well-Defined, Organic Nanoenvironments in Water: The Hydrophobic Effect Drives a Capsular Assembly. *J. Am. Chem. Soc.* **2004**, *126*, 11408-11409.

39. Ramamurthy, V., Photochemistry within a Water-Soluble Capsule. *Acc. Chem. Res.* **2015**, *48*, 2904-2917.

40. Kaanumalle, L., S.; Gibb, C., L. D.; Gibb, B., C.; Ramamurthy, V., A Hydrophobic Nanocapsule Controls the Photophysics of Aromatic Molecules by Suppressing Their Favored Solution Pathways. *J. Am. Chem. Soc.* **2005**, *127*, 3674-3675.

41. Mukherjee, P.; Das, A.; Sengupta, A.; Sen, P., Bimolecular Photoinduced Electron Transfer in Static Quenching Regime: Illustration of Marcus Inversion in Micelle. *J. Phys. Chem. B* **2017**, *121*, 1610-1622.

42. Choudhury, R.; Barman, A.; Prabhakar, R.; Ramamurthy, V., Hydrocarbons Depending on the Chain Length and Head Group Adopt Different Conformations within a Water-Soluble Nanocapsule: 1h Nmr and Molecular Dynamics Studies. *The Journal of Physical Chemistry B* **2013**, *117*, 398-407.

43. Frisch, M.; Trucks, G.; Schlegel, H.; Scuseria, G.; Robb, M.; Cheeseman, J.; Scalmani, G.; Barone, V.; Mennucci, B.; Petersson, G., Gaussian 09, Revision D. 01. Gaussian, Inc., Wallingford CT: 2009.

44. Becke, A. D., Density-Functional Thermochemistry. I. The Effect of the Exchange-Only Gradient Correction. *The Journal of Chemical Physics* **1992**, *96*, 2155-2160.

45. Francl, M. M.; Pietro, W. J.; Hehre, W. J.; Binkley, J. S.; Gordon, M. S.; DeFrees, D. J.; Pople, J. A., Self-Consistent Molecular Orbital Methods. Xxiii. A Polarization-Type Basis Set for Second-Row Elements. *The Journal of Chemical Physics* **1982**, *77*, 3654-3665.

46. Wang, J.; Wolf, R. M.; Caldwell, J. W.; Kollman, P. A.; Case, D. A., Development and Testing of a General Amber Force Field. *Journal of Computational Chemistry* **2004**, *25*, 1157-1174.

47. Trott, O.; Olson, A. J., Autodock Vina: Improving the Speed and Accuracy of Docking with a New Scoring Function, Efficient Optimization, and Multithreading. *Journal of Computational Chemistry* **2010**, *31*, 455-461.

48. Hess, B.; Kutzner, C.; Van Der Spoel, D.; Lindahl, E., Gromacs 4: Algorithms for Highly Efficient, Load-Balanced, and Scalable Molecular Simulation. *Journal of Chemical Theory and Computation* **2008**, *4*, 435-447.

49. Case, D. A.; Cheatham, T. E.; Darden, T.; Gohlke, H.; Luo, R.; Merz, K. M.; Onufriev, A.; Simmerling, C.; Wang, B.; Woods, R. J., The Amber Biomolecular Simulation Programs. *Journal of Computational Chemistry* **2005**, *26*, 1668-1688.

50. Price, D. J.; Brooks III, C. L., A Modified Tip3p Water Potential for Simulation with Ewald Summation. *The Journal of Chemical Physics* **2004**, *121*, 10096-10103.

51. Miyamoto, S.; Kollman, P. A., Settle: An Analytical Version of the Shake and Rattle Algorithm for Rigid Water Models. *Journal of Computational Chemistry* **1992**, *13*, 952-962.

52. Hess, B.; Bekker, H.; Berendsen, H. J.; Fraaije, J. G., Lincs: A Linear Constraint Solver for Molecular Simulations. *Journal of Computational Chemistry* **1997**, *18*, 1463-1472.

53. Krieger, E.; Vriend, G., Yasara View—Molecular Graphics for All Devices—from Smartphones to Workstations. *Bioinformatics* **2014**, *30*, 2981-2982.

54. Pettersen, E. F.; Goddard, T. D.; Huang, C. C.; Couch, G. S.; Greenblatt, D. M.; Meng, E. C.; Ferrin, T. E., Ucsf Chimera—a Visualization System for Exploratory Research and Analysis. *Journal of Computational Chemistry* **2004**, *25*, 1605-1612.

55. Valiev, M., et al., Nwchem: A Comprehensive and Scalable Open-Source Solution for Large Scale Molecular Simulations. *Computer Physics Communications* **2010**, *181*, 1477-1489.

56. Yanai, T.; Tew, D. P.; Handy, N. C., A New Hybrid Exchange-Correlation Functional Using the Coulomb-Attenuating Method (Cam-B3lyp). *Chemical Physics Letters* **2004**, *393*, 51-57.

57. Grimme, S.; Ehrlich, S.; Goerigk, L., Effect of the Damping Function in Dispersion Corrected Density Functional Theory. *Journal of Computational Chemistry* **2011**, *32*, 1456-1465.

58. Grimme, S.; Antony, J.; Ehrlich, S.; Krieg, H., A Consistent and Accurate Ab Initio Parametrization of Density Functional Dispersion Correction (Dft-D) for the 94 Elements H-Pu. *Journal of Chemical Physics* **2010**, *132*.

59. Jayaraj, N.; Zhao, Y.-P.; Parthasarathy, A.; Porel, M.; Liu, R. S. H.; Ramamurthy, V., Nature of Supramolecular Complexes Controlled by the Structure of the Guest Molecules: Formation of Octa Acid Based Capsuleplex and Cavitandplex. *Langmuir* **2009**, *25*, 10575-10586.

60. Porel, M.; Jayaraj, N.; Kaanumalle, L. S.; Maddipatla, M. V. S. N.; Parthasarathy, A.; Ramamurthy, V., Cavitand Octa Acid Forms a Nonpolar Capsuleplex Dependent on the Molecular Size and Hydrophobicity of the Guest. *Langmuir* **2009**, *25*, 3473-3481.

61. Chandross, E. A.; Dempster, C. J., Excimer Fluorescence and Dimer Phosphorescence from a Naphthalene Sandwich Pair. *J. Am. Chem. Soc.* **1970**, *92*, 704-706.

62. Chandross, E. A.; Ferguson, J., Mixed Excimer Fluorescence; the Importance of Charge-Transfer Interaction. *J. Chem. Phys.* **1967**, *47*, 2557-2560.

63. Koti, A. S. R.; Krishna, M. M. G.; Periasamy, N., Time-Resolved Area-Normalized Emission Spectroscopy (Tranes): A Novel Method for Confirming Emission from Two Excited States. *J. Phys. Chem. A* **2001**, *105*, 1767-1771.

64. Koti, A. S. R.; Periasamy, N., Application of Time Resolved Area Normalised Emission Spectroscopy to Multicomponent Systems. . *J. Chem. Phys.* **2001**, *115*, 7094-7099.

65. Periasamy, N.; Koti, A. S. R., Time Resolved Fluorescence Spectroscopy: Tres and Tranes. *Proc. Indian Natn. Acad. Sci.* **2003**, *69*, 41-48.

66. Birks, J. B.; Lumb, M. D.; Munro, I. H.; Flowers, B. H., 'Excimer' Fluorescence V. Influence of Solvent Viscosity and Temperature. *Proc. R. Soc. Lond. A* **1964**, *280*, 289-297.

67. Ni, T.; Melton, L. A., Two-Dimensional Gas-Phase Temperature Measurements Using Fluorescence Lifetime Imaging. *Appl. Spectrosc.* **1996**, *50*, 1112-1116.

68. Wells, M. R.; Melton, L. A., Temperature Measurements of Falling Droplets. *J. Heat Transfer* **1990**, *112*, 1008-1013.

69. Lou, J.; Hatton, T. A.; Laibinis, P. E., Fluorescent Probes for Monitoring Temperature in Organic Solvents. *Anal. Chem.* **1997**, *69*, 1262-1264.

70. Das, A.; Kamatham, N.; Raj, A. M.; P.Sen; Ramamurthy, V., Marcus Relationship Maintained During Ultrafast Electron Transfer across a Supramolecular Capsular Wall. *J. Phys. Chem. A* **2020**, *124*, 5297-5305.

71. Gao, Y.; Liu, H.; Zhang, S.; Gu, Q.; Shen, Y.; Ge, Y.; Yang, B., Excimer Formation and Evolution of Excited State Properties in Discrete Dimeric Stacking of an Anthracene Derivative: A Computational Investigation. *Phys.Chem. Chem. Phys.* **2018**, *20*, 12129-12137.

72. Otolski, C. J.; Raj, M. A.; Ramamurthy, V.; Elles, C. G., Spatial Confinement Alters the Ultrafast Photoisomerization Dynamics of Azobenzenes. *Chem. Sci.* **2020**, *11*, 9513-9523.

73. Das, A.; Sharma, G.; Kamatham, N.; Prabhakar, R.; Sen, P.; Ramamurthy, V., Ultrafast Solvation Dynamics Reveal the Octa Acid Capsule's Interior Dryness Depends on the Guest. *J. Phys. Chem. A* **2019**, *123*, 5928-5936.

74. Raj, A. M.; Gaurav Sharma; Prabhakar, R.; Ramamurthy, V., Xenon Triggers Phosphorescence at Room Temperature from Encapsulated Pyrene. *J. Phys. Chem. A* **2019**, *123*, 9123-9131.

TOC Graphics